A constructive framework for discovery, design, and classification of volumetric Bravais weaves

Tolga T. Yildiz [ID][a], Alice C. Niemeyer [ID][b], Vinayak R. Krishnamurthy [ID][a,c] and Ergun Akleman [ID][a,d,*]

[a]Department of Computer Science and Engineering, Texas A&M University, College Station, TX 77840, USA
[b]Chair of Algebra and Representation Theory, RWTH Aachen University, Pontdriesch 10-16, 52062 Aachen, Germany
[c]J. Mike Walker '66 Department of Mechanical Engineering, Texas A&M University, College Station, TX 77840, USA
[d]Visual Computing and Computational Media Section, School of Performance, Visualization and Fine Arts, Texas A&M University, College Station, TX 77840, USA
*To whom correspondence should be addressed: Email: ergun.akleman@gmail.com
Edited By Michael Harris

Abstract

Woven fabrics have a long history of study across the fields of art, mathematics, and mechanics. While weaves with symmetries in $\mathbb{R}^2$ have been extensively formalized, classified, and characterized, a systematic framework for representing and designing weaves in $\mathbb{R}^3$ remains absent. Despite their relevance to engineering applications—particularly in composite materials—volumetric weaves are often designed in an ad hoc manner, typically by stacking planar weaves and introducing trivial thread connections along the stacking axis. In this article, we establish a formal framework for volumetric weaves by defining them through the isometries of Bravais lattices and their corresponding Voronoi cells in $\mathbb{R}^3$. This approach provides a structured description of the design space for a specific family of volumetric weaves, which we call volumetric Bravais weaves. As an example of volumetric Bravais weaves, we analyze, *cubic primitive weaves* (cP-weaves) in detail as the simplest example within the volumetric Bravais weave framework. This example demonstrates how volumetric Bravais weave structures naturally emerge from 3D lattice isometries. Furthermore, we show that all possible cP-weaves can be systematically generated using a set of cP lattice isometries and cube isometries. Our findings reveal that even just the space of cP-weaves is at least one order of magnitude larger than that of conventional two-way 2-fold weaves, highlighting the potential of our approach for expanding the design space of volumetric weaves.

Keywords: volumetric weaves, cP-weaves, woven fabrics, material design, Wigner-Seitz cells

Significance Statement

Volumetric weaves offer exceptional structural versatility, making them promising candidates for lightweight, high-strength materials in aerospace, architecture, and advanced manufacturing. However, their systematic design and classification have remained an open challenge. This work introduces a mathematical framework that enables the precise representation, enumeration, and discovery of a specific class of volumetric weaves, which we call volumetric Bravais weaves. By providing a structured methodology, our approach significantly expands the design space of volumetric weaves and unlocks new opportunities for engineered materials, offering pathways for tailored mechanical properties, optimized manufacturing, and novel structural applications.

Introduction

Volumetric fabrics have been widely explored in engineering and material sciences, particularly in the context of fabric-reinforced composites, where woven or knitted binding threads secure structural elements such as rigid bars or fiber reinforcements. The uniquely interwoven geometry of these structures has enabled a wide range of material applications, from textile manufacturing (1) to engineering composites and tissue engineering (2). These studies often rely on numerical simulations to analyze mechanical properties and manufacturability constraints (3–17). For a recent comprehensive review, see Hasan et al. (18).

A critical knowledge gap in the utilization of volumetric woven geometries for architected materials and composites comes from the lack of principled approaches for the design of such geometries. As a result, the current state of the art, by and large, uses ad hoc design principles to design volumetric woven structures and primarily focuses on the physical realization and mechanical characterization of volumetric fabrics. In contrast, our work takes a complementary perspective by examining volumetric weaves through the lens of discrete mathematics and symmetry and focuses on developing a framework to systematically classify these weaves using a subset of 3D lattice symmetries. This symmetry-based perspective enables us to identify structural patterns that may not be immediately evident through purely physical or numerical approaches.

The primary contribution of this article is the development of a systematic and versatile representation for volumetric weaves, which we call volumetric Bravais weaves (Fig. 1). This representation facilitates a broad range of applications, including the discovery of novel weave structures and the formalization of periodic volumetric weaving using combinatorial and algebraic principles. Our approach provides a unified framework for classifying, designing, and exploring volumetric weaving patterns in a structured manner.

As a demonstration of the framework's expressiveness, we enumerate specific volumetric weaves with minimal periodicity constraints and establish lower bounds on the number of possible volumetric weave structures. While these results are not the central focus of our work, they serve as evidence of the generality and scalability of our methodology. By leveraging this representation, we show that volumetric weaves can be systematically generated and classified, significantly expanding the scope of possible weave architectures. Beyond a mathematically grounded design methodology, this framework has broader implications for fields such as fiber arts, textile engineering, and computational design.

Background on volumetric weaves

Much of the earlier work on volumetric weaves implicitly relies on mathematical frameworks originally developed for planar weaves, such as isonemal fabrics (19–22). Consequently, existing approaches often extend planar weave symmetries by layering or stacking them in three dimensions, without establishing an independent formalism for volumetric weaves (23). While recent studies have acknowledged the role of space groups and crystallographic lattices in describing periodic entanglements (24, 25) and their embeddings in hyperbolic spaces (26, 27), explicit representations that allow different local thread configurations (see Fig. 1b) for volumetric weaves remain absent. Additionally, modular design strategies have been explored (16, 28), yet a comprehensive mathematical framework for representing the full weave configuration and design space is still lacking.

Mathematical studies of knots have long been well-developed, while weaving, despite its structural complexity, has received comparatively less formal mathematical attention. One possible reason for this is the historical perception of weaving as a craft rather than a rigorous mathematical subject. However, recently, there has been strong interest in the crystallography community in the formalization of volumetric weaves, aiming to bridge this gap by providing a structured and systematic approach. For instance, there has been some exploration of the rod packing problem (29, 30) and the symmetries of rod packings (31), which bear similarities to volumetric weaves (see Fig. 2). However, rod packings by definition do not consider local configurations, as the rod unit that tiles the space does not have different configurations.

Another recent discovery on periodic entanglements (26, 27, 32–34) proposes embedding weave strands in triply periodic surfaces and hyperbolic planes. In these works, the local embedding is determined by mapping the hyperbolic plane ($\mathbb{H}^2$) to the triply periodic surface ($\mathbb{E}^3$), which defines the path that the strand follows. These structures, called entanglements, generate different classes of periodic volumetric structures, including invariant rod packings, intersecting filament axes, tangled weaves, and looped filaments. These structures explore remarkable periodic entanglements and provide a way to parametrize periodic structures using a single hyperbolic plane. However, these works primarily focus on creating repeating unit structures. In fact, we observe that these resulting structures are derivable within the design space of our volumetric Bravais weaves, specifically cP-weaves (see Fig. 2b) and have a rich design space (see Fig. 2c). Moreover, these structures span only a limited subspace of what is possible within the larger design space. This is because they do not consider the local configuration of each thread and instead use the same unit structure generated by the mapping to define the geometry. In contrast, by assigning each unit cell different thread structures and allowing all Wigner–Seitz cells as unit cells, we significantly extend the design space.

Volumetric Bravais weaves

In this article, we introduce volumetric Bravais weaves, a systematic and formal approach to defining a specific family of volumetric weaves using 3D lattice structures. By formulating these weaves intrinsically within 3D crystallographic lattices, we provide a rigorous framework that enables a structured exploration of their mathematical properties. Our primary focus is on establishing the fundamental formalisms that describe the design space of volumetric weaves, rather than exhaustively characterizing their mechanical behavior. This framework enables us to use different 3D tessellations to construct volumetric weaves (see Fig. 1d and e). To illustrate the power of this approach, we investigate cubic primitive weaves (cP-weaves) as the simplest example within this formalism. By doing so, we reveal a broad and previously underexplored design space, laying the groundwork for future investigations into the mathematical and physical properties of volumetric weaves. Our key contributions can be as follows:

1. **Lattice-based mathematical framework**: We introduce a mathematically constructive framework for defining volumetric weaves based on 3D Bravais lattices and Wigner–Seitz cells.
2. Using this framework, we analyze a specific subset of volumetric Bravais weaves, namely, cP-weaves and plain cP-weaves, to demonstrate the power of overall framework.
3. **Generality of framework**: Our mathematical approach subsumes the space of 2D weaves and rod packings (Fig. 2), demonstrating its generality.
4. **Bounds for the space of cP-weaves**: We provide lower bounds for the number of possible cP-weave configurations given a defined number of elements in a domain.
5. **Enumeration**: We enumerate plain cP-weaves up to an $8 \times 8 \times 8$ domain.
6. **Enumeration algorithm for plain cP-weaves**: We develop a formal algorithm to enumerate plain cP-weaves efficiently.
7. **Algorithms for designing cP-weaves**: We present new computational design strategies for constructing cP-weaves.

Definition of volumetric Bravais weaves

A *thread* is the image of an embedding of $\mathbb{R}$ into $\mathbb{R}^3$. An *entanglement* is a disjoint union of possibly infinitely many threads and
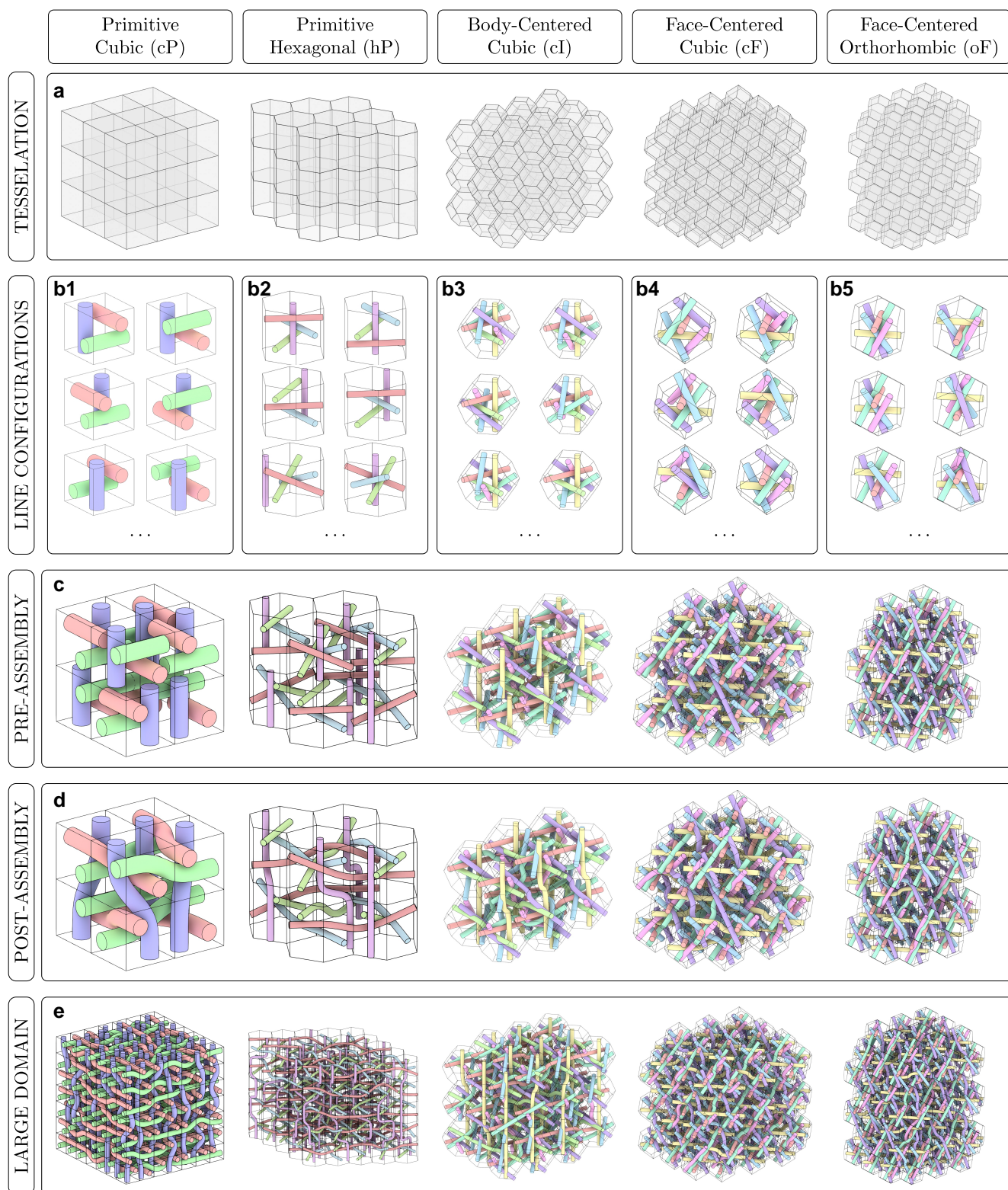
Fig. 1. Examples of volumetric Bravais weaves: a) Five topologically distinct Wigner–Seitz cells serve as the fundamental building blocks of volumetric weaves, allowing for variations in both cell types and thread counts. b) Demonstrates different possible arrangements of threads within each cell, defining local thread configuration. c) Presents the preassembly configurations of local structures for each cell, while d) illustrates the process of assembling these local threads. Finally, e) showcases large-domain examples, highlighting how threads aligned in the same direction are interconnected and smoothed.

loops in $\mathbb{R}^3$. There is rich literature on entanglements; see Refs. (26, 27, 32, 34). In this article, we consider very special entanglements, called *weaves*, as defined below.

Although it is possible to define volumetric weaves even more generally, here we focus on weaves in which the points where the threads meet (crossing points) are evenly spaced in $\mathbb{R}^3$, and
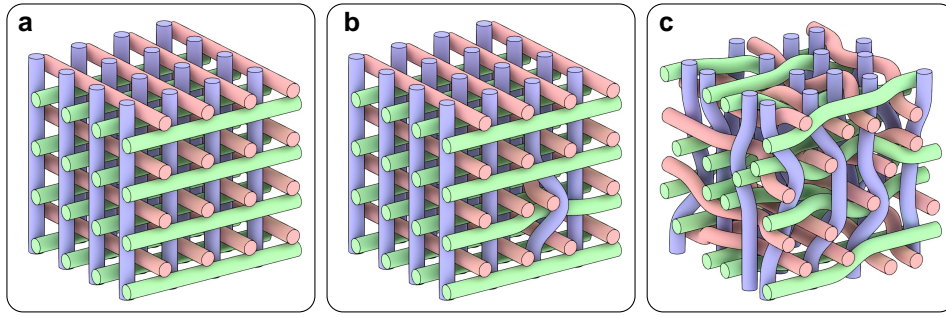
Fig. 2. Our volumetric Bravais weaves encompass rod packings as a special case, as shown in a), while maintaining full local control over individual thread configurations, as shown in b). This approach enables a significantly expanded design space for volumetric weaves, allowing for diverse and customizable local configurations, as shown in c).

at each "crossing point" the number of threads meeting at this point is constant. Let $B := \{v_1, v_2, v_3\}$ be the basis for $\mathbb{R}^3$. Define $\mathcal{L}(\{v_1, v_2, v_3\}) = \{iv_1 + jv_2 + kv_3 \mid i, j, k \in \mathbb{Z}\}$. Then, $\mathcal{L}(B)$ is a full Bravais lattice in $\mathbb{R}^3$ and, as usual, we denote a vector $iv_1 + jv_2 + kv_3 \in \mathcal{L}(\{v_1, v_2, v_3\})$ by (i, j, k). Given a lattice $\mathcal{L}(B)$, a cell containing exactly one lattice point, called the *Wigner–Seitz cell* or the *Voronoi cell*, can be defined by considering all points in $\mathbb{R}^3$ closest to the lattice point. The translated copies of these cells fill the entire space.

DEFINITION 1   Let $B = \{v_1, v_2, v_3\}$ be the basis for $\mathbb{R}^3$. Suppose that C is a Voronoi cell of $\mathcal{L}(B)$, and let $\ell \in \mathbb{Z}$ be the number of configurations of n skew lines, where n is equal to the number of faces of C. A *volumetric Bravais weave* with basis B is a map $V : \mathcal{L}(B) \to \{1, \ldots, \ell\}$. For $(i, j, k) \in \mathcal{L}(B)$, the value $V(i, j, k)$ is called the *configuration of the threads* meeting in (i, j, k).

REMARK 1   Skew lines are a set of lines that do not intersect and are not parallel to each other (35). For example, the two lines through opposite edges of a regular tetrahedron are skew lines. Similarly, three nontouching edges of a cube define three skew lines.

REMARK 2   A volumetric Bravais weave with basis B can be thought of as an entanglement of threads obtained from lines that meet at lattice points by diverting the lines around the intersection point.

1. Any line is parallel to a vector from the center of the Voronoi cell to the nearest lattice point. A line passes through exactly two faces of the Voronoi cell.
2. Any two different lines can only meet at a point in $\mathcal{L}(B)$.
3. For each $(i, j, k) \in \mathcal{L}(B)$, the number n of pairwise nonparallel lines meeting in (i, j, k) is equal to half of the number of faces of the Voronoi cell.
4. Observe that the Voronoi cell has the same symmetries as the lattice.
5. In a woven structure the lines are replaced by threads, and at the intersection points of lines the threads are diverted to be locally an arrangement of skew lines. The value $V(i, j, k)$ allows us to arrange the n threads around (i, j, k) in a well-defined entanglement, see Proposition 1 for details.

Representation of cP-weaves as GF(2)^3 group on lattice cells

This definition is very general and allows us to define very interesting volumetric Bravais weaves. In this article, we focus on

one particular Wigner–Seitz cell, namely the cube. The reason for this focus is that this cell is easy to understand, allowing us to highlight the difference between volumetric and plane weaves. Already with this example, we are able to demonstrate the vast potential volumetric Bravais weaves possess. We will consider other Wigner–Seitz cells in a forthcoming publication. Suppose henceforth that the basis B consists of the 3 unit vectors of $\mathbb{R}^3$, and thus our lattice is $\mathbb{Z}^3$ and a Voronoi cell C is a cube. This lattice corresponds to the primitive cubic lattice in the crystallography context, and we call these weaves *primitive cubic weaves* (cP-weaves). In this case, the configurations of skew lines passing through two faces of C each can be parameterized by choosing three edges of C such that no two have a common vertex (35). We can therefore identify $V(i, j, k)$ with a cube C with three distinguished edges. These configuration of skew lines are closely related to the invariant cubic rod packings (31) in a sense that the tiling of these skew lines in the space would create a basis for rod packings as can be seen in Fig. 2a. This formulation of the volumetric weaves subsumes the rod packing definition and create different structures from the initial rod packing (see Fig. 2).

We are particularly interested in weaves that display some non-trivial symmetry. When considering different symmetric weaves that can be obtained by Definition 1, we need to distinguish two different types of symmetry, the first type of symmetry is the group of isometries of the unit cell, as the cell geometry helps us to identify the local configurations (see Figs. 3 and 4). The second type of symmetry is the symmetry group of the Bravais lattice, which supports the translation of the weave to obtain itself again.

A cP-weave consists of skew lines arranged in a cP lattice (Fig. 1a) where each group of skew line segments defines the local configuration of the threads (Fig. 1b1) within the Voronoi cell, i.e. cube. Each pair of threads in the cube has an order. When all the rank orders are combined, we get a *configuration* of the cell. From the definition of cP-weave, the configurations of a cell can be identified with three distinguished edges no two of which share a vertex, which leads to eight different cell configurations (see Fig. 3).

Representing a volumetric Bravais weave involves three steps: (i) Establishing an initial rank-order representation of threads within the unit cell. (ii) Encoding all possible configurations of the threads in the unit cell. (iii) Defining a lattice system to encode and represent local configurations for each cell. If the encoding in (ii) is consistent with the symmetry operations of the unit cell, it enables the development of a simple and elegant method for representing line configurations within a given unit cell.

In the case of cP-weaves, the mirror symmetries of the cube naturally generate all possible line configurations. Mirror
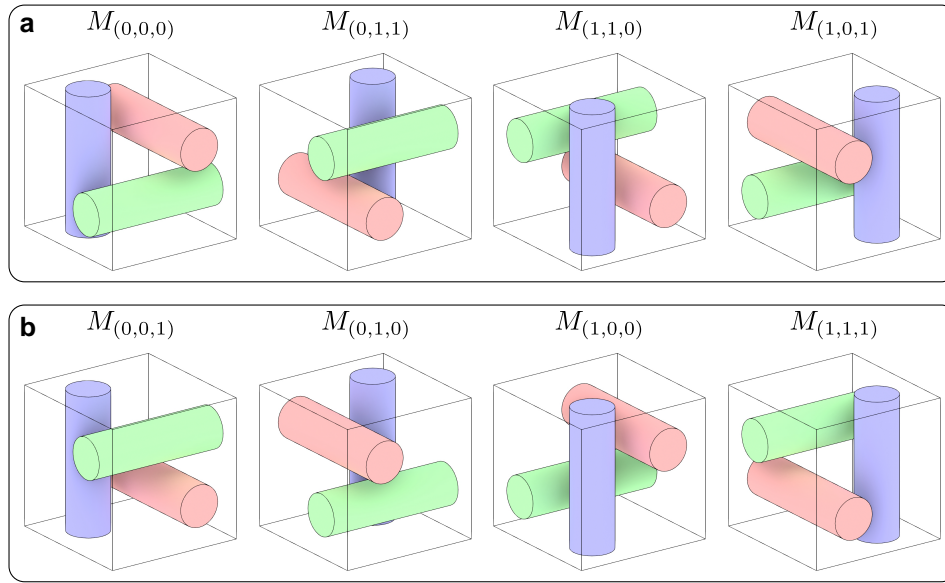
Fig. 3. Using the thread configurations in a) and b), we can construct a variety of cP-weaves as can be seen from Fig. 1d and e. Configurations can be separated into two groups where each group only consists of thread configurations that can be obtained with rotations from one configuration of the same group. Take group a) as an example, each of the configurations are just a rotation of other thread configurations from group a).

operations can be represented using mirror matrices of the following form:

$$M_{(x,y,z)} = \begin{pmatrix} (-1)^x & 0 & 0 \\ 0 & (-1)^y & 0 \\ 0 & 0 & (-1)^z \end{pmatrix}, \quad (1)$$

where x, y, $z \in \{0, 1\}$ and the multiplication of two mirror matrices can be expressed as:

$$M_{(x_1,y_1,z_1)} M_{(x_2,y_2,z_2)} = M_{(x_1+x_2,y_1+y_2,z_1+z_2)}, \quad (2)$$

where $+$ is modulo 2 addition. Notably, this set of matrices forms a group with identity $M_{(0,0,0)}$ that is isomorphic to the additive group $GF(2)^3$, where matrix multiplication corresponds to element-wise addition modulo 2.

We assume that the initial thread configuration is chosen arbitrarily and corresponds to the identity matrix $M_{(0,0,0)}$. The other configurations, obtained by applying the mirror matrix $M_{(x,y,z)}$ to this initial configuration, can be labeled accordingly, as illustrated in Fig. 3. By exploiting the group isomorphism mentioned above, we can thus represent the possible thread configurations of a cP-weave using the elements of $GF(2)^3$.

Since each Bravais lattice point can be assigned a distinct configuration, a general cP-weave can be viewed as a mapping from lattice points to elements of $GF(2)^3$, formally expressed as: $V : \mathbb{Z}^3 \to GF(2)^3$.

Construction of cP-weaves in translation cells

The key idea in the construction of cP-weaves is to identify configuration changes from one cell to another in all three directions. This approach is fundamentally different from planar weaves, where such changes do not need to be explicitly identified. To facilitate this, we introduce the concept of a discrete derivative. Given a cP-weave $V : \mathbb{Z}^3 \to GF(2)^3$, we can now define discrete derivatives in all three, i.e. x, y, and z, directions as $\delta_x V = V(n+1, m, k) - V(n, m, k)$, $\delta_y V = V(n, m+1, k) - V(n, m, k)$, and $\delta_z V = V(n, m, k+1) - V(n, m, k)$, respectively. The discrete derivatives for the derivatives in the x direction are shown in Fig. 5.

PROPOSITION 1 Let there be a cP-weave V with $N \times M \times K$ a translation cell W. Then the geometry of the V, i.e. the configuration of the skew lines, can be constructed from an $N \times M \times K$ cubic array with entries in the vector space $GF(2)^3$.

Proof. Each cell of W encodes a unit cube with three distinct skew line segments that lie parallel to the principal axis of the cubic primitive Bravais lattice; these three skew lines are treated as a local portion of the threads in W. We may assume that the specific embeddings of these skew lines are the following:

1. $x = \overline{X_0 X_1}$, $X_0 = (-0.5, -y_0, -z_0)$, $X_1 = (0.5, -y_0, -z_0)$
2. $y = \overline{Y_0 Y_1}$, $Y_0 = (-x_0, -0.5, z_0)$, $Y_1 = (-x_0, 0.5, z_0)$
3. $z = \overline{Z_0 Z_1}$, $Z_0 = (x_0, y_0, -0.5)$, $Z_1 = (x_0, y_0, 0.5)$.

This constitutes the base configuration of threads where the pairwise rank orders are given as $r_{(x,y)} = 1$ denoting that the x thread has a higher rank than y within the xy plane projection, $r_{(y,z)} = 1$ denoting that the y thread has a higher rank than z within the yz plane projection and $r_{(x,z)} = 1$ denoting that the x thread has the higher rank than z within xz plane projection.

As shown in Ref. (35), there are two distinct configurations of these three skew line segments if we only have one set of three skew lines. But in our cP-weaves we use different sets of three skew lines at different places in space, e.g. lattice points, which distinguishes the orientation of the threads and results in eight different configurations, since each $r_{(i,j)} \in GF(2)$ giving $2 \times 2 \times 2 = 8$.

Then in each cell $C = W(i, j, k)$, we can use a binary triplet $(r_{(y,z)}(i, j, k), r_{(x,z)}(i, j, k), r_{(x,y)}(i, j, k)) \in GF(2)^3$ to represent the pairwise ranking orders which span the entire configuration space for the local thread configuration. This rank-order representation can be realized with the mirror matrix applied to the base configuration as discussed before. Thus creating a unique representation of the cP-weave as the collection of all $W(i, j, k) = (r_{yz}(i, j, k), r_{(xz)}(i, j, k), r_{(xy)}(i, j, k))$ resulting in a $GF(2)^3$ valued cubic array.
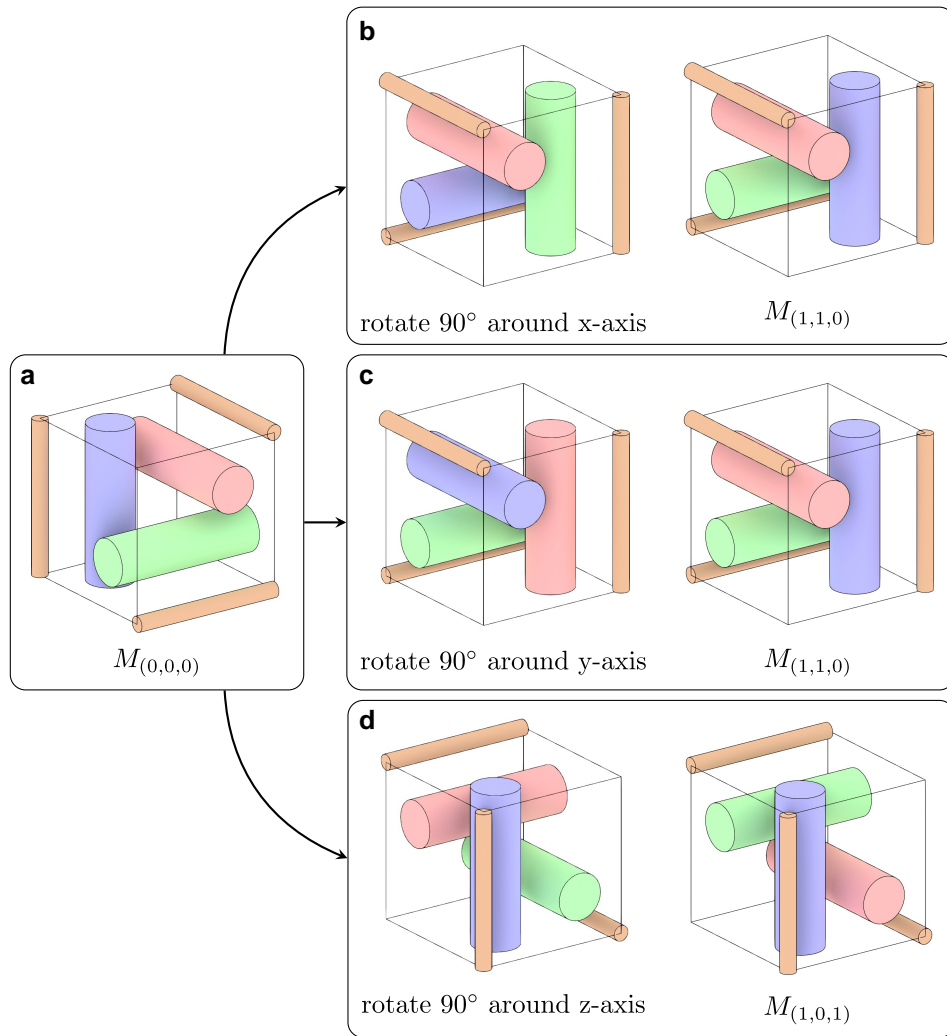
Fig. 4. One of the Voronoi cell from the eight fundamental cubes in Fig. 3 is given in (a). After a rotation operation along the principal axes in $\mathbb{R}^3$, each cell is transformed into the cells in (b) which corresponds to another configuration in Fig. 3 that is shown in (c). Using this property we can map a configuration in regular cP-weave V_1 to the rotated V_1 and find an isometry between the weaves.

REMARK 3 The resulting virtual construction consists of piecewise linear curves, as shown in Figs. 5 and 1c. Any two line segments between two neighboring cubes are connected with short line segments at the interface of the two neighboring cubes. These short line segments do not intersect with other skew lines, since the others do not intersect with the face separating the two cubes. This guarantees that the resulting threads do not intersect with each other.

REMARK 4 There is still a caveat, since we smooth these piecewise linear curves for virtual construction as shown in Fig. 6. For smoothing, it is better to use a parametric formula that satisfies partition of unity such as B-splines and Bezier curves (36, 37), then we can use piecewise linear curves as control points of this parametric system. Since the resulting smooth curves always stay in the convex hull of local control points, it is easy to avoid intersections. In our implementations, we used Non-Uniform Rational B-Spline curves (38).

Design space of cP-weaves

Recall that the group of isometries that leave a Bravais lattice invariant is a crystallographic group G and as such is a discrete subgroup of the Euclidean group E(3). The Voronoi cell is a translation cell of the lattice and is mapped by elements of G to another translation cell. The symmetry group of the orthogonal lattice with standard basis (i.e. the cubic primitive lattice) and cubic Voronoi cell C is $\mathbb{Z}^3 \rtimes O(C)$, where $O(C)$ denotes the symmetry group of the cube and has order 24.

DEFINITION 2 Let V be a cP-weave with lattice $\mathcal{L}(B)$. An automorphism of V is a lattice isometry α of $\mathcal{L}(B)$ such that $V(\alpha(i, j, k)) = \alpha(V(i, j, k))$ for all $(i, j, k) \in \mathcal{L}(B)$, where $\alpha(V(i, j, k))$ is the image of the cube $V(i, j, k)$ under α. We denote the group of automorphisms of V by Aut(V).

Isometric properties of cP-weaves

To study the isometric properties of cP-weaves, we used a specific subset, which we call regular cP-weaves.

DEFINITION 3 A *regular cP-weave* is a cP-weave such that there is a $M \times M \times M$ cubic translation cell W such that V is generated from W by translations along vectors of length M along the standard basis. In this case, Aut(W) denotes the set of lattice isometries fixing W and Aut(W) ≤ Aut(V).

Fig. 5. All possible $\delta_x V$ values for a neighborhood visualized with the single initial configuration $V(0, 0, 0) = (0, 0, 0)$ (rightmost cell in each cell pair) and $V(1, 0, 0) = V(0, 0, 0) + \delta_x V$ (leftmost cell in each cell pair). Note that the connections here are not postprocessed to show the initial geometry of local weaves and how connections are formed between cells. These connections ensure that the threads do not intersect each other.
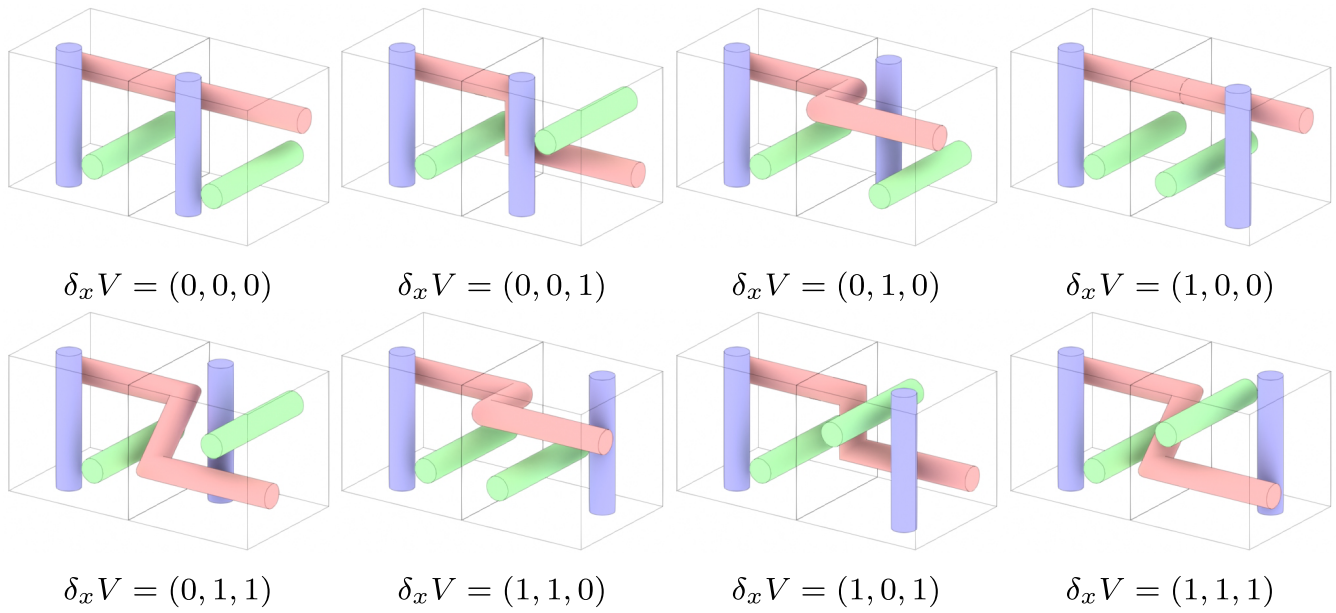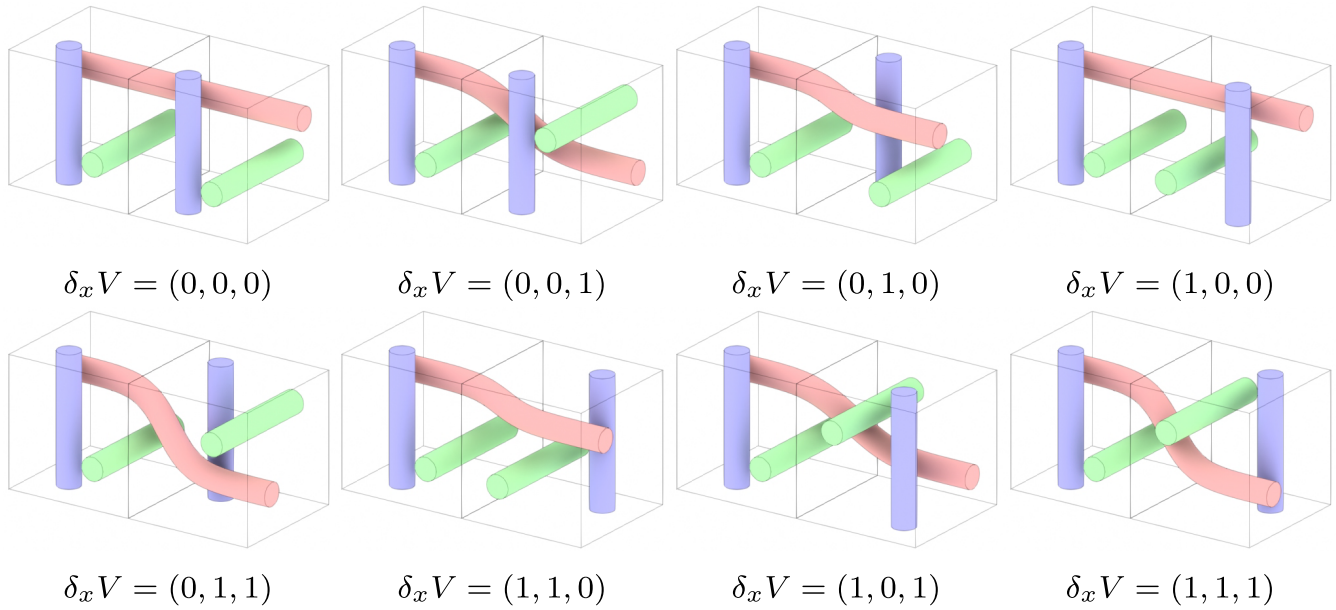

Fig. 6. Smoother versions of threads in Fig. 5 with all possible $\delta_x V$ values for a neighborhood visualized with a single initial configuration $V(0, 0, 0) = (0, 0, 0)$ (rightmost cell in each cell pair) and $V(1, 0, 0) = V(0, 0, 0) + \delta_x V$ (leftmost cell in each cell pair). Note that the connections are smoothed to show how the final connections are formed between the cells. These smoothed curves do not intersect since we become sure that the convex hulls of the local control points do not intersect.

The most important property of the regular cP-weaves for our purposes is that they can be rotated in all three directions, which makes it easier to study isometry properties.

DEFINITION 4 A *regular plain cP-weave* is a regular cP-weave for which any two-way 2-fold weave in a plane orthogonal to any of the coordinate axes is a plain weave with respect to the remaining two coordinates (see Fig. 7).

We are also interested in regular plain cP-weaves and their representations. Our aim is to show that volumetric weaves facilitate

a far larger design space than two-way 2-fold weaves. Although two-way 2-fold weaves only admit one type of plain weave, we show that the number of regular plain cP-weaves grows exponentially in the size of a cubic translation cell.

We begin by introducing a very convenient and compact way of representing regular plain cP-weaves.

PROPOSITION 2 Let W be an $M \times M \times M$ translation cell for a regular plain cP-weave V. Let $v_0 = (x_0, y_0, z_0) = W(1, 1, 1)$. Then, there are vectors d_x, d_y, $d_z \in GF(2)^M$ such that W, and thus also V, is uniquely determined by (v_0, d_x, d_y, d_z).
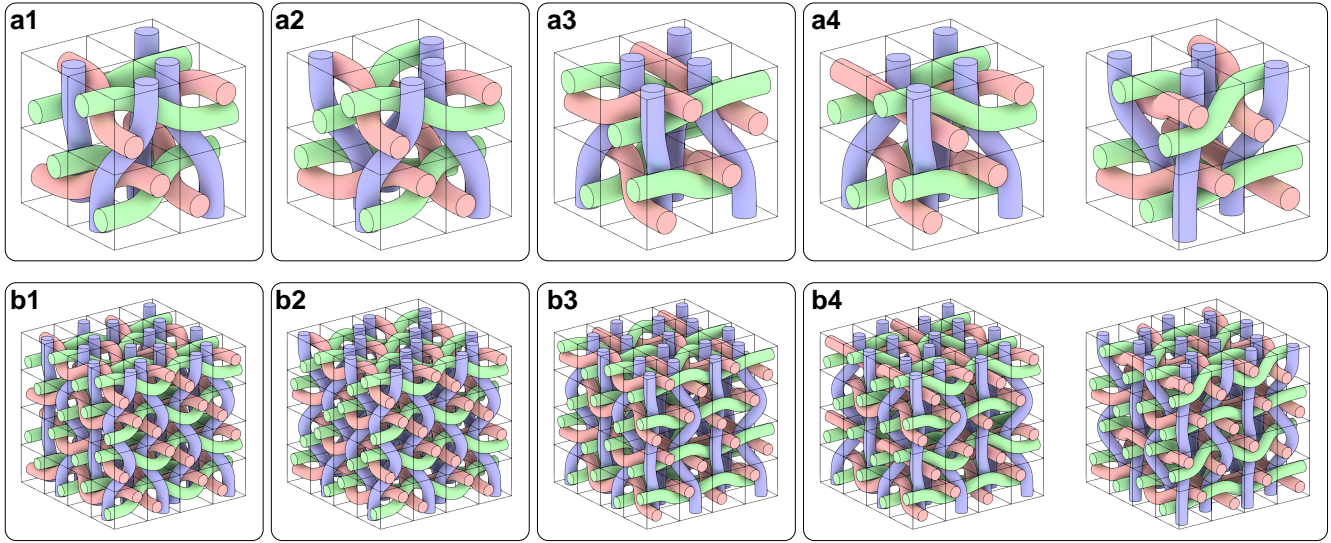
Fig. 7. One interesting subset of cP-weaves is *regular plain* cP-weaves (see Definition 4). In these weaves, threads are always changing their rank orders from one cell to the other. The number of different regular plain cP-weaves depends on the size of the domain(see Proposition 4). In a1–a4, we show all possible regular plain cP-weaves for $2 \times 2 \times 2$ cellular domain. b1–b4) are extended version of the a1–a4) respectively, i.e. $2 \times 2 \times 2$ domain is repeated to get $4 \times 4 \times 4$ cP-weave. Note that counting different weaves depends on the allowed symmetry operations as well. Here, we grouped the weaves based on cellular translation, rotation and mirror operations which allows for four different $2 \times 2 \times 2$ regular plain cP-weave. If we remove mirror operation then the group a4) separates into two groups(right and left images), this means that all weaves in a1–a3) are self-chiral.

Proof. Note that a regular plain cP-weave has to satisfy that in transitioning from $W(i, j, k)$ to a neighboring cube, say to $W(i + 1, j, k)$, the two pairs of threads in the x, y-plane as well as in the x, z-plane change ranking order. In other words, $\delta_x W(i, j, k) = W(i + 1, j, k) - W(i, j, k) = (a, 1, 1)$ for some $a \in GF(2)$. This means for the derivatives and i, j, k $\in \{1, \ldots, M - 1\}$

$$\begin{aligned} \delta_x W(i, j, k) &= W(i + 1, j, k)) - W(i, j, k) = (a_{ijk}, 1, 1), \\ \delta_y W(i, j, k) &= W(i, j + 1, k) - W(i, j, k) = (1, b_{ijk}, 1), \\ \delta_z W(i, j, k) &= W(i, j, k + 1) - W(i, j, k) = (1, 1, c_{ijk}), \end{aligned} \quad (3)$$

for $a_{ijk}, b_{ijk}, c_{ijk} \in GF(2)$.

We now show that $a_{ijk} = a_{ij'k'}$ for all i, j, k, j', k' $\in \{1, \ldots, M\}$. In other words, the derivative $\delta_x W(i, j, k)$ only depends on i, the derivative $\delta_y W(i, j, k)$ only depends on j, and the derivative $\delta_z W(i, j, k)$ only depends on k.

Let i, j, k $\in \{1, \ldots, M\}$. We compare two ways of reaching $W(i + 1, j + 1, k)$ from $W(i, j, k)$, namely

$$\begin{aligned} &W(i, j, k) + (a_{i,j,k}, 1, 1) + 1, b_{i+1,j,k}, 1) \\ &= W(i + 1, j, k) + (1, b_{i+1,j,k}, 1) = W(i + 1, j + 1, k), \\ &W(i, j, k) + (1, b_{i,j,k}, 1) + (a_{i,j+1,k}, 1, 1) \\ &= W(i, j + 1, k) + (a_{i,j+1,k}, 1, 1) = W(i + 1, j + 1, k). \end{aligned}$$

Subtracting these two equations we obtain

$$(a_{i,j,k}, 1, 1) + (1, b_{i+1,j,k}, 1) = (1, b_{i,j,k}, 1) + (a_{i,j+1,k}, 1, 1)$$

or $(a_{i,j,k}, b_{i+1,j,k}, 1) = (a_{i,j+1,k}, b_{i,j,k}, 1)$. This shows that $a_{i,j,k} = a_{i,j+1,k}$ and $b_{i+1,j,k} = b_{i,j,k}$. An analogous argument shows that the same holds for $c_{i,j,k}$. Therefore, we denote $a_{i,j,k}$ simply by a_i and the derivatives are $\delta_x W(i, j, k) = (a_i, 1, 1)$, $\delta_y W(i, j, k) = (1, b_j, 1)$, and $\delta_z W(i, j, k) = (1, 1, c_k)$, where i, j, k $\in \{1, \ldots, M - 1\}$ and $a_i, b_j, c_k \in GF(2)$. Furthermore, define a_M, b_M, and c_M in GF(2) by $W(M, j, k) - W(1, j, k) = (a_M, 1, 1)$, and $W(i, M, k) - W(i, 1, k) = (1, b_M, 1)$, $W(i, j, M) - W(i, j, 1) = (1, 1, c_M)$.

Since the cP-weaves are regular, translating V along any of the axes M steps leaves V invariant. A translation of V along the x-axis by one step corresponds to applying the cyclic permutation $(1, \ldots, M)$ to $d_x W$. This shows that $\sum_{i=1}^{M-1} a_i = a_M$, $\sum_{i=1}^{M-1} b_i = b_M$, $\sum_{i=1}^{M-1} c_i = c_M$, since $W(M, j, k) + d_x W(a_M, 1, 1) = W(1, j, k)$.

The cP-weave V is therefore uniquely determined by $v_0 := W(1, 1, 1)$ and the three vectors $d_x = (a_1, \ldots, a_M)$, $d_y = (a_1, \ldots, a_M)$, and $d_z = (a_1, \ldots, a_M)$.

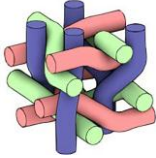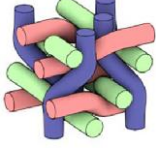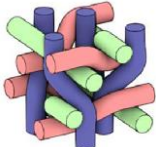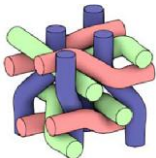## Design space for repeating $GF(2)^3$ vector space

The following propositions shows that volumetric weaves open up a huge design space. Considering regular cP-weaves with an $M \times M \times M$ translation cell, allows to design a number of different weaves that grow exponentially in M. This is true even for regular plain cP-weaves, where in the 2D case we have only one weave up to automorphisms. The following propositions provide a lower bound for the design space. To obtain a lower bound, we consider the threads of different kinds in cP-weaves (three orthogonal threads) to be same such that we can use the automorphisms of the cube to map one kind of thread to another.

PROPOSITION 3 The number of regular cP-weaves generated by an $M \times M \times M$ translation cell is at least $\frac{1}{48} 2^{3(M^3 - \log_2(M))}$.

Proof. Observe first that the full automorphism group of the primitive cubic lattice is $\mathbb{Z}^3 \rtimes O_h$, where O_h denotes the full octahedral group, which is also the group of isometries of a cube. Now suppose that W is an $M \times M \times M$ translation cell and define $G = (C_M \times C_M \times C_M) \rtimes O_h$, where C_M denotes the cyclic group of order M. Then, the automorphism group of the weave generated by W is the subgroup Aut(W) of G consisting of all weave automorphisms. The action of an element in $C_M \times C_M \times C_M$ on W corresponds to a translation of the translation cell W. Let Ω denote the set of all possible configurations in $GF(2)^3$ that W can take. In the case of a regular cP-weave, $|\Omega| = 8^{M^3}$.

Given two such configurations, the weaves they generate might lie in the same orbit under G. In fact, the different weaves are in

Table 1. Representatives of orbits on $2 \times 2 \times 2$ regular plain cP-weaves under full lattice isometry group $\mathbb{Z}^3 \rtimes O_h$

Orbit Representative W	Visualization of W	|Aut (W)|	Orbit Length
[10 : 00 : 10]		16	24
[00 : 01 : 00]		16	24
[01 : 10 : 01]		48	8
[11 : 11 : 00]		48	8
		Total	64

bijection to the orbits of G on Ω. The action of an element of O_h on W corresponds to applying a cube symmetry to W.

We obtain the lower bound for the number of regular cP-weaves by dividing $|\Omega|$ by the length of the longest orbit of G on Ω. Since the length of any orbit divides $|G|$, it is less than $|G|$, whence a lower bound for the number of different weaves is $\frac{|\Omega|}{|G|}$. For regular cP-weaves this yields the lower bound $\frac{8^{M^3}}{M^3 \cdot 48} = \frac{1}{48} 2^{3(M^3 - \log_2(M))}$.

PROPOSITION 4   The number of regular plain cP-weaves generated by an $M \times M \times M$ translation cell is at least $\frac{1}{48} 2^{3(M - \log_2(M))}$.

Proof. The proof is similar to the one provided for Proposition 3. We will utilize the full automorphism groups of cubic primitive lattice and the full octahedral group. By Proposition 2, a regular plain cP-weave with translation cell W is uniquely described by a tuple (v_0, d_x, d_y, d_z), where $v_0 \in \mathrm{GF}(2)^3$ and $d_x, d_y, d_z \in \mathrm{GF}(2)^M$ such that $\sum_{i=1}^{M-1} a_i = a_M$, $\sum_{i=1}^{M-1} b_i = b_M$, $\sum_{i=1}^{M-1} c_i = c_M$, hence in this case $|\Omega| = 8 \cdot 2^{3(M-1)} = 2^{3M}$.

Given two such configurations, the weaves they generate might lie in the same orbit under G and different weaves are in bijection to the orbits of G on Ω.

We obtain the lower bound for the number of regular plain cP-weaves by dividing $|\Omega|$ by the length of the longest orbit of G on Ω. Since the length of any orbit divides $|G|$, it is less than $|G|$, whence a lower bound for the number of different weaves is $\frac{|\Omega|}{|G|}$. For regular plain cP-weaves it yields $\frac{2^{3M}}{M^3 \cdot 48} = \frac{1}{48} 2^{3(M - \log_2(M))}$.

Our enumeration of periodic volumetric weaves and the derived lower bounds should be understood as applications of our representation rather than as standalone results. These findings validate the expressiveness of our framework, demonstrating its ability to systematically encode a vast number of volumetric weaves within a structured combinatorial space.

The lower bound we establish on the number of possible volumetric weaves confirms that our representation provides access to a significantly larger design space than previously considered. By applying our systematic encoding, we illustrate how the classification and discovery of volumetric weaves become more structured and computationally feasible.

Designing weaves based on primitive cubic lattices

A weave based on primitive cubic lattices (cP-weave) with an $M \times N \times K$ translation cell can be represented by 8^{MNK} values in GF(2). The design space of these cP-weaves increases exponentially with each number increase in the domain size as shown in Proposition 3. With this many number of parameters, it is not feasible to determine each configuration of the cell in the lattice with manual entries. In this section, we will provide different strategies that can be employed to design cP-weaves such that configurations can be generated with an algorithm.

Design of the cP-weaves with constraints

For some weave types, we can further constrain the representation. Constraints can be introduced with a neighborhood definition which could be expressed in terms of derivative definitions as shown in (3). The constraint given in Eq. 3 results in a plain cP-weave and the simple representation of a regular plain cP-weave has been proved in Proposition 2. Note that each cell in this representation has a triplet of values which can be treated as a binary number. Also note that each variable in this array (not the entries), determines whether the layer of fabric is mirrored in the direction of the variable, i.e. x_1 is controlling the y–z mirror of second y–z planar weave in the structure. Then a compact representation of an $M \times N \times K$ plain cP-weave is the following collection of binary variables:
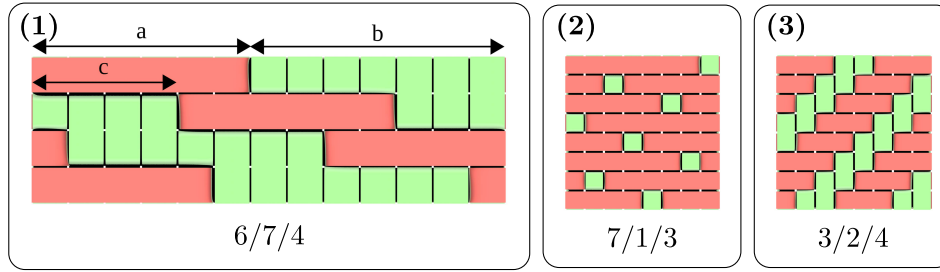
Fig. 8. $a/b/c$ notation(1) is one of the simplest representation for biaxial weaves. Satins(2) and Twills(3) can be represented by this notation.

$$\mathbf{W} = [x_0 \ldots x_{M-1} : y_0 \cdots y_{N-1} : z_0 \cdots z_{K-1}]. \tag{4}$$

This reduces the number of parameters from $3(M*N*K)$ to $M + N + K$ for plain cP-weaves. Similar constraint definitions can be used to define different cP-weaves such as twills, this approach can be empowered with cellular automata (39) by defining a behavior for a neighborhood of $p \times q \times t$ and this domain can generate different configurations to define the cP-weaves.

In Table 1, we show one representative W for each orbit of the group $\mathbb{Z}^3 \rtimes O_h$ of lattice isometries on the set of $2 \times 2 \times 2$ translation cells of regular plain cP-weaves with together with the order of the automorphism group Aut(W) of W.

Shifting strategy

The shifting strategy has been used for designing 2D weaves before (see Fig. 8), which requires a binary local configuration encoding and three parameters to generate entries for the representation. $a/b/c$ notation for 2D weaves consists of a binary representation of the local rank order (0 or 1) and three parameters a, b, c. Then, the planar weave is given by the following equation:

$$W(i, j) = \begin{cases} 0 & i + j*c \bmod(a + b) < a \\ 1 & i + j*c \bmod(a + b) \geq a. \end{cases} \tag{5}$$

To apply the same shifting strategy to cP-weaves, we reduce the number of configurations from 8 to 2 by choosing two configurations such that $c_1 - c_2 = (1, 1, 1)$ where $c_1, c_2 \in GF(2)^3$. This enables us to use the shifting strategy to determine the crossings as this strategy uses only two configurations and it ensures that the crossing happens in every direction at the location specified by the shifting strategy. $a/b/c$ can define only a single layer; however, to be able to define multiple layers we need to add another shift variable for the layer index, let that shift variable be d. Then, we can populate the $M \times N \times K$ array that represents the cP-weave W with the following equation:

$$W(i, j, k) = \begin{cases} c_1 & i + j*c + k*d \bmod(a + b) < a \\ c_2 & i + j*c + k*d \bmod(a + b) \geq a \end{cases} \tag{6}$$

which uses two independent shifts in y and z directions. This enable us to design weaves that has different type of planar weaves in three different constant planes of the cP-weave (see Fig. 9).

Generalization of shifting strategy for volumetric weaves

Now, let us assume that a square $N \times M$ two-way 2-fold weave is given. Now, note that this two-way 2-fold fabric is given by a matrix of ones and zeros. Let us assume that this matrix is in the $z = 0$ plane. To obtain the $z = k$ plane, we cyclically shift this matrix in x-direction ks_0 amount and y-direction ks_1 amount. Our corollary

is that if two number pairs are relatively prime, then the cP-weave will consist of x-constant, y-constant, and z-constant planes. These two number pairs are (a) N and $s_0 + s_1$; and (b) M and $s_0 + s_1$. For such types of fabrics, we can use the notation $(N, s_0) \times (M, s_1)$ following Grunbaum and Shephard's notation of (n, s) (see Figs. 10 and 11).

Pattern generation for other volumetric Bravais weaves using cubic arrays of configurations

We represent $M \times N \times K$ translation cells of cP-weaves using a cubic array with entries. This digital representation with a cubic array of configurations allows for a structured approach to modeling any volumetric Bravais weaves. In other words, this representation extends beyond cP-weaves. Any of the other four distinct cases of volumetric Bravais weaves (i.e. hP, cI, cF, and oF) can also be effectively described using cubic arrays of configurations, where the cubic arrays still correspond to translational $M \times N \times K$ cells. This capability comes directly from the core strength of the Bravais-based framework, as every lattice point in a Bravais lattice can be expressed—by definition—through a set of discrete translation operations in 3D space: $\mathbf{p} = a_0 \vec{v}_0 + a_1 \vec{v}_1 + a_2 \vec{v}_2$, where the a_i's are arbitrary integers and $\vec{v}_0$, $\vec{v}_1$, and $\vec{v}_2$ are three linearly independent vector in $\mathbb{R}^3$.

The only distinction with cP-weaves is that for the four other Wigner–Seitz cases, the configurations will not be represented by $GF(2)^3$. Nevertheless, shifting strategies remain applicable to all cases, regardless of the specific nature of the mathematical representations of configurations. In other words, shift operations can be universally employed to generate repeating patterns that correspond to any volumetric Bravais weave.

An additional advantage of shift operations is that they establish connections with familiar planar weave structures, such as plain, twill, and satin. However, it is crucial to recognize that this connection is not a necessity. For volumetric weaves, there is no fourth dimension into which they could "fall off," meaning that 2D patterns hold no fundamental significance beyond their historical legacy and familiarity. In reality, the choice of patterns can be entirely arbitrary.

Furthermore, we anticipate that statistical distributions of configuration variations will have a direct impact on the physical properties of these weaves, making this an important avenue for future investigation.

Discussion

A fundamental question in volumetric weaving is why 2D weaving is universally present across cultures, while 3D weaving remains largely absent in traditional practices. This asymmetry likely stems from human dexterity constraints, as weaving in two
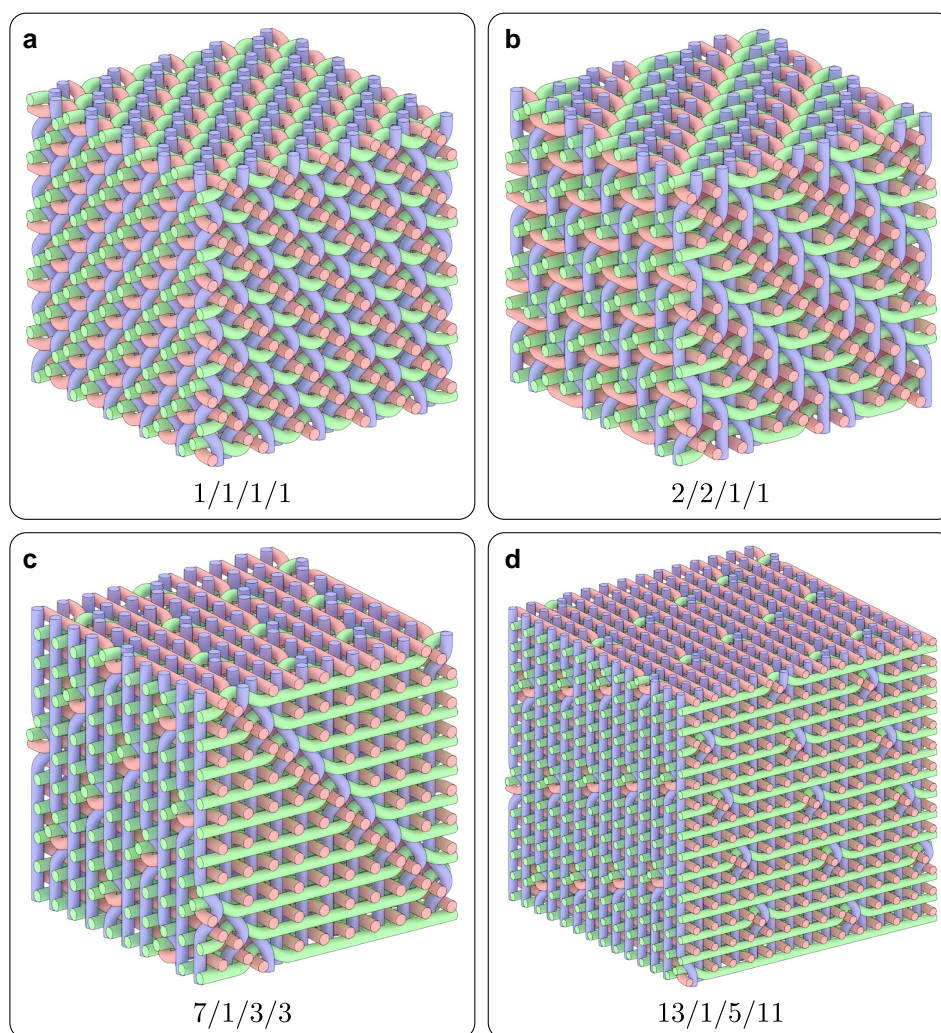
Fig. 9. Volumetric fabrics can be designed with $a/b/c/d$ notation. We have used volumes that are larger than the fundamental region to visually demonstrate differences in periodic structures.

dimensions allows for the use of the third dimension to manipulate threads, whereas full-3D weaving requires simultaneous interlacing in a way that exceeds manual coordination. However, modern fabrication technologies, can provide an alternative means of constructing volumetric woven structures without the need for direct thread manipulation. This perspective highlights the relevance of our approach, which formalizes 3D weaving as a mathematical framework, independent of fabrication constraints, offering new opportunities for computational fabrication, composite materials, and advanced manufacturing techniques.

A key advantage of our approach is that it introduces a generalized representation that makes the classification, design, and discovery of volumetric weaves significantly more accessible. Unlike previous methods that rely on manually defined weave types, our methodology provides a formal structure for analyzing volumetric weaves as combinatorial objects. This structured representation not only offers an improved way to study existing volumetric weaves but also provides a systematic approach for identifying previously unknown configurations.

We would like to emphasize that our approach provides a new algebraic alternative to the well-established representation of 2D fabrics introduced by Grünbaum and Shephard (19–22). Our

formulation allows for a structured and mathematically rigorous treatment of woven structures. Specifically, our method enables the representation of two-way 2-fold and three-way 3-fold weaves by utilizing 2D Bravais lattices. These weaves can be classified based on their underlying symmetry properties, where tetragonal primitive (tp) lattices correspond to two-way 2-fold weaves, while hexagonal primitive (hp) lattices are used to define three-way 3-fold weaves. This distinction highlights the fundamental role that lattice structures play in the mathematical characterization of fabric patterns. By leveraging algebraic techniques, our approach not only provides an alternative perspective but also extends the applicability of lattice-based fabric representations. This allows for a more systematic exploration of fabric designs while maintaining consistency with classical textile classifications.

We also want to point out that there still exist a significant difference in 2D and 3D woven structures. One of the main contributions of Grünbaum and Shephard was to observe that weaving patterns that appear to be perfectly linked by visual inspection may not produce links that can make the woven structure hang together (19–22, 40–42). In other words, the resulting structures could come apart in pieces. They called a weaving structure a fabric only if it is hanging together. We want to point out that the concept of "hanging together" is not relevant for volumetric weaves since there is no fourth

a Fabric 4-1-1 $(4, 1) \times (4, 3)$

b Fabric 5-1-1 $(5, 1) \times (5, 2)$

c Fabric 8-5-2 $(8, 2) \times (8, 3)$

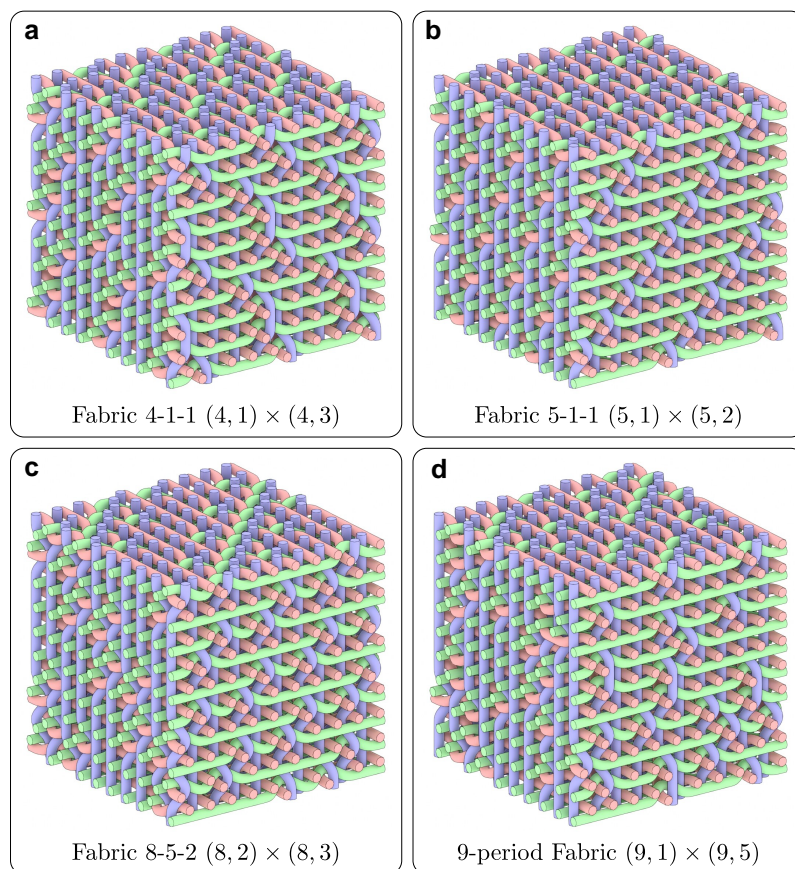**d** 9-period Fabric $(9, 1) \times (9, 5)$

Fig. 10. This figure provides some volumetric fabrics that can be given in $(N, s_0) \times (M, s_1)$ notation. We have used volumes that are larger than the fundamental region to visually demonstrate differences in periodic structures.
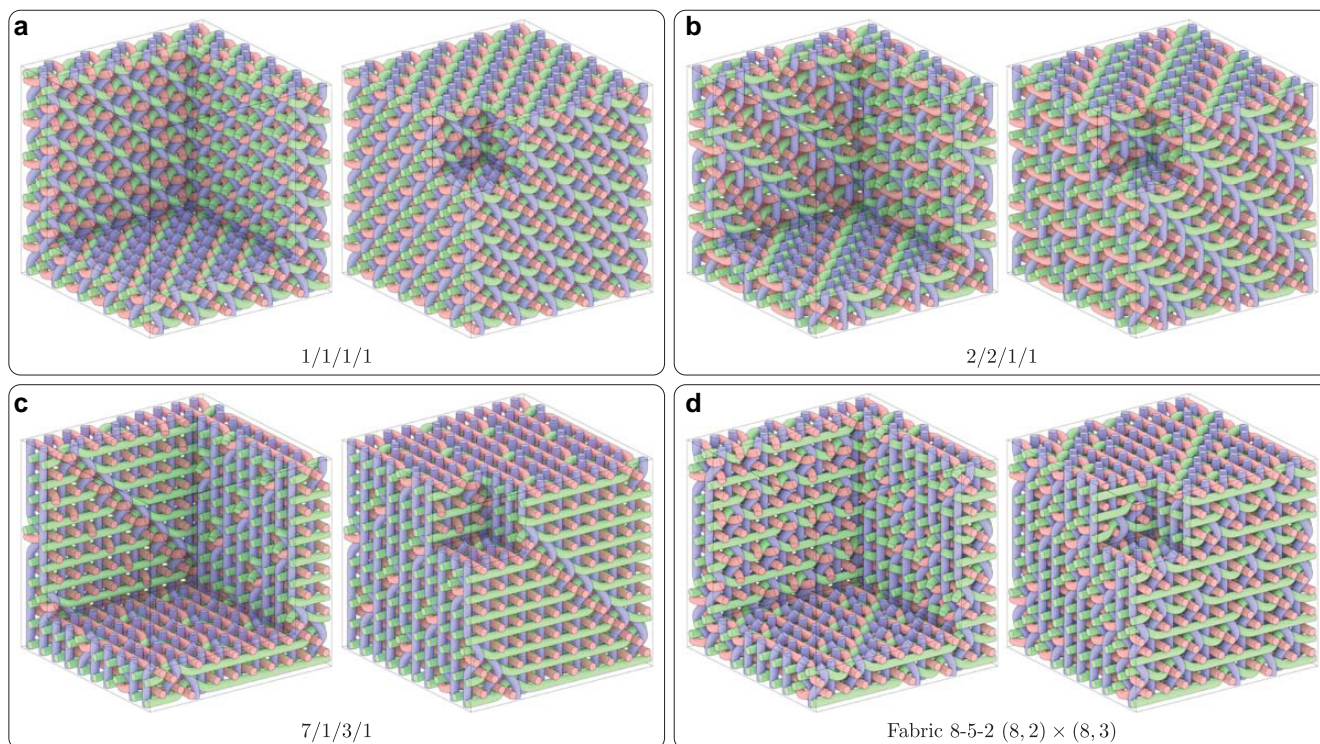

a 1/1/1/1

b 2/2/1/1

c 7/1/3/1

d Fabric 8-5-2 $(8, 2) \times (8, 3)$

Fig. 11. This figure shows the internal structure of these 3D volumetric fabrics. a–c) are slices for ABC notated fabrics and d) is the slicing for shift constructed volumetric fabric 8-5-2 in $(8, 2) \times (8, 3)$ configuration.
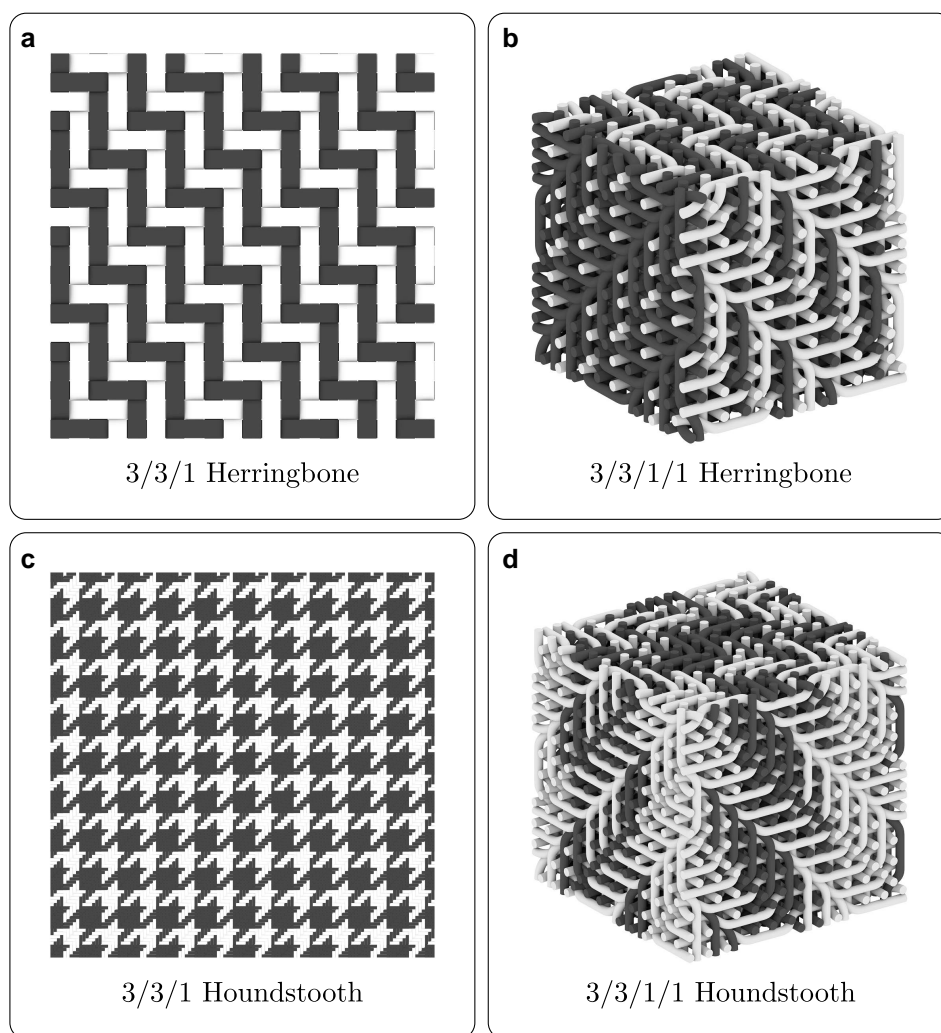
Fig. 12. This figure demonstrates the effect of coloring for the same weave. In this case, we used a relatively simple, 3/3/1 twill, and corresponding 3/3/1/1 cP-weave just to demonstrate how the number of possibilities increases by using different materials.

dimension into which it could fall off. While it is intuitively observed that removing a thread from a volumetric weave requires pulling it lengthwise, we do not formally claim that volumetric weaves "hang together" in the same sense as 2D fabrics. Instead, we limit our discussion of this property to cases where it applies within 2D slices of volumetric structures.

The interplay between weaving and mathematical structures extends beyond volumetric weaves. Related work on fiber arts, such as hyperbolic crochet pioneered by Daina Taimina, highlights how topological principles can be physically realized through structured materials (43). Similar to hyperbolic crochet, volumetric weaves provide a tangible way to explore mathematical properties through textile structures, reinforcing the deep and often overlooked connection between mathematics and fiber arts.

Conclusion and future work

In this article, we present a constructive mathematical framework for the effective representation of a special class of volumetric weaves. Our framework provides access to a vast and scalable design space, enabling algorithmic exploration and potential optimizations for various engineering applications. The enumeration and lower bounds presented in this article demonstrate the versatility of our approach, showcasing its applicability beyond established weave families. Future research can build upon this representation to facilitate automated design, classification, and refinement of all volumetric Bravais weaves, with significant potential in computational design and materials science.

In practical applications, this work has the potential to contribute to various engineering fields. We envision applications in engineered structures such as convective heat exchangers (44), composites (45, 46), and lattice materials (47). Another promising research direction is exploring alternative methods beyond enumerating topologically distinct cases to achieve desired properties. For instance, coloring threads can generate a wide range of patterns. In twill alone, patterns such as herringbone, houndstooth, serge, sharkskin, flannel, cavalry, chino, covert, denim, drill, and gabardine can be obtained (48). This approach can also be leveraged to create diverse textures (48–50) (see Fig. 12 for examples of planar and volumetric weaves).

Volumetric fabrics have been explored in various engineering applications to enhance the strength and mechanical performance of composite materials. For example, volumetric weaves can be embedded as reinforcements in concrete structures, acting as a rebar-like framework to improve load distribution and fracture resistance. Similarly, volumetric fabrics are used in aerospace and wind energy applications, where their lightweight yet strong properties contribute to structural efficiency in aircraft

components and wind turbine blades. While this article primarily focuses on the geometric construction and classification of volumetric weaves, the presented framework has the potential to be extended for engineering applications where mechanical properties play a critical role.

By establishing a formalized approach to volumetric weaves, this research not only contributes to mathematical and computational design but also opens avenues for broader engagement in material sciences, engineering, and textile arts. The mathematical study of woven structures holds significant potential for public engagement, bridging abstract mathematical principles with real-world applications in an intuitive and visually compelling way.

Funding

Author Contributions

T.Y. implemented the system and created all images. A.N. provided formal proofs and definitions for cP-weaves and uniqueness of a regular cP-weave. E.A. conceived the initial idea and its formalism, wrote the initial draft of the article. V.K. identified $GF(2)^3$ fundamental group and its operations. All authors reviewed the manuscript.

Data Availability

There are no data underlying this work.

References

1. Hu J. *Structure and mechanics of woven fabrics*. Elsevier, 2004.
2. Moutos FT, Freed LE, Guilak F. 2007. A biomimetic three-dimensional woven composite scaffold for functional tissue engineering of cartilage. *Nat Mater*. 6(2):162–167.
3. Bilisik K. 2012. Multiaxis three-dimensional weaving for composites: a review. *Text Res J*. 82(7):725–743.
4. Cox BN, Dadkhah MS, Morris WL, Flintoff JG. 1994. Failure mechanisms of 3D woven composites in tension, compression, and bending. *Acta Metall Mater*. 42(12):3967–3984.
5. El-Dessouky HM, Saleh MN. 3D woven composites: from weaving to manufacturing. In: *Recent developments in the field of carbon fibers*. IntechOpen, 2018. p. 51.
6. Guénon VA, Chou T-W, Gillespie JW. 1989. Toughness properties of a three-dimensional carbon-epoxy composite. *J Mater Sci*. 24(11):4168–4175.
7. Khokar N. 1996. 3D fabric-forming processes: distinguishing between 2D-weaving, 3D-weaving and an unspecified non-interlacing process. *J Text Inst*. 87(1):97–106.
8. Khokar N. 2001. 3D-weaving: theory and practice. *J Text Inst*. 92(2):193–207.
9. Kuo W-S, Cheng-Po Chen T-HK. 2007. Effect of weaving processes on compressive behavior of 3D woven composites. *Compos Part A Appl Sci Manuf*. 38(2):555–565.
10. Mishra R, Militky J, Gupta N, Pachauri R, Behera BK. 2015. Modelling and simulation of earthquake resistant 3D woven textile structural concrete composites. *Compos B Eng*. 81(2):91–97.
11. Mohamed MH. 1990. Three-dimensional textiles. *Am Sci*. 78(6):530–541.
12. Mohamed MH, Bogdanovich AE. 2009. Comparative analysis of different 3D weaving processes, machines and products. In: *Proceedings of the 17TH International Conference on Composite Materials (ICCM-17)*. International Committee on Composite Materials (ICCM). p. 27–31.
13. Perera YS, Muwanwella RMHW, Fernando PR, Fernando SK, Jayawardana TSS. 2021. Evolution of 3D weaving and 3D woven fabric structures. *Fash Text*. 8(1):1–31.
14. Ren Y, et al. 2021. 3D weaving with curved ribbons. *ACM Trans Graph (TOG)*. 40(4):1–15.
15. Takahashi H, Kim J. 2019. 3D printed fabric: techniques for design and 3D weaving programmable textiles. In *Proceedings of the 32nd Annual ACM Symposium on User Interface Software and Technology*. Association of Computing Machinaries (ACM). p. 43–51.
16. van Schuylenburch DWPF. 1993. Three-dimensional woven structure, Aug 1990. Patent No. US5263516A, Filed May 5th., 1990, Issued Nov. 23rd.
17. Wu R, et al. 2020. Weavecraft: an interactive design and simulation tool for 3D weaving. *ACM Trans Graph*. 39(6):210–1.
18. Hasan KMF, Horváth PG, Alpár T. 2021. Potential fabric-reinforced composites: a comprehensive review. *J Mater Sci*. 56(26):14381–14415.
19. Grunbaum B, Shephard G. 1980. Satins and twills: an introduction to the geometry of fabrics. *Math Mag*. 53(3):139–161.
20. Grunbaum B, Shephard G. 1985. A catalogue of isonemal fabrics. *Ann N Y Acad Sci*. 440(1):279–298.
21. Grunbaum B, Shephard G. 1986. An extension to the catalogue of isonemal fabrics. *Discrete Math*. 60:155–192.
22. Grünbaum B, Shephard GC. 1988. Isonemal fabrics. *Am Math Monthly*. 95(1):5–30.
23. Stig F, Hallström S. 2012. Spatial modelling of 3D-woven textiles. *Compos Struct*. 94(5):1495–1502.
24. Liu Y, O'Keeffe M, Treacy MMJ, Yaghi OM. 2018. The geometry of periodic knots, polycatenanes and weaving from a chemical perspective: a library for reticular chemistry. *Chem Soc Rev*. 47(12):4642–4664.
25. O'Keeffe M, Treacy MMJ. 2020. Crystallographic descriptions of regular 2-periodic weavings of threads, loops and nets. *Acta Crystallogr A*. 76(2):110–120.
26. Evans ME, Robins V, Hyde ST. 2013. Periodic entanglement II: weavings from hyperbolic line patterns. *Acta Crystallogr A*. 69(3):262–275.
27. Evans ME, Robins V, Hyde ST. 2015. Ideal geometry of periodic entanglements. *Proc R Soc A: Math Phys Eng Sci*. 471(2181):20150254.
28. Lord EA, Ranganathan S. 2006. Truchet tilings and their generalisations. *Resonance*. 11(6):42–50.
29. O'Keeffe M, Andersson S. 1977. Rod packings and crystal chemistry. *Acta Crystallogr A*. 33(6):914–923.
30. Rosi NL, et al. 2005. Rod packings and metal-organic frameworks constructed from rod-shaped secondary building units. *J Am Chem Soc*. 127(5):1504–1518.
31. O'Keeffe M, Plévert J, Teshima Y, Watanabe Y, Ogama T. 2001. The invariant cubic rod (cylinder) packings: symmetries and coordinates. *Acta Crystallogr A*. 57(1):110–111.
32. Andriamanalina T, Evans ME, Mahmoudi S. 2025. Diagrammatic representations of 3-periodic entanglements. *Topol Appl*. 368(12):109346.
33. Evans ME, Hyde ST. 2015. Periodic entanglement III: tangled degree-3 finite and layer net intergrowths from rare forests. *Acta Crystallogr A*. 71(6):599–611.

34 Evans ME, Robins V, Hyde ST. 2013. Periodic entanglement I: networks from hyperbolic reticulations. *Acta Crystallogr A.* 69(3): 241–261.

35 Viro J, Viro O. 2006. Configurations of skew lines, arXiv, arXiv:math/0611374, https://doi.org/10.48550/arXiv.math/0611374, preprint: not peer reviewed.

36 Bartels RH, Beatty JC, Barsky BA. *An introduction to splines for use in computer graphics and geometric modeling*. Morgan Kaufmann, 1995.

37 Cohen E, Riesenfeld RF, Elber G. *Geometric modeling with splines: an introduction*. AK Peters/CRC Press, 2001.

38 Piegl L, Tiller W. *The NURBS book*. Springer Science & Business Media, 1996.

39 Bays C. 1988. Classification of semitotalistic cellular automata III three dimensions. *Complex Syst.* 2:235–254.

40 Griswold RE. 2004. Color complementation, Part 1: Color-alternate weaves. Web Technical Report, Computer Science Department, University of Arizona.

41 Griswold RE. 2004. From drawdown to draft: a programmer's view. Web Technical Report, Computer Science Department, University of Arizona.

42 Griswold RE. 2004. When a fabric hangs together (or doesn't). Web Technical Report, Computer Science Department, University of Arizona.

43 Taimina D. *Crocheting adventures with hyperbolic planes: tactile mathematics, art and craft for all to explore*. CRC Press, 2018.

44 Avila-Marin AL, Fernandez-Reche J, Casanova M, Caliot C, Flamant G. 2017. Numerical simulation of convective heat transfer for inline and stagger stacked plain-weave wire mesh screens and comparison with a local thermal non-equilibrium model. *AIP Conf Proc.* 1850(1):030003.

45 Gereke T, Cherif C. 2019. A review of numerical models for 3D woven composite reinforcements. *Compos Struct.* 209:60–66.

46 Li M, Wang S, Zhang Z, Wu B. 2009. Effect of structure on the mechanical behaviors of three-dimensional spacer fabric composites. *Appl Compos Mater.* 16(1):1–14.

47 Salari-Sharif L, *et al.* 2018. Damping of selectively bonded 3D woven lattice materials. *Sci Rep.* 8(1):14572.

48 Feijs LMGGeometry and computation of houndstooth (pied-de-poule). In: Bosch R, McKenna D, Sarhangi R, editors. *Proceedings of bridges 2012: mathematics, music, art, architecture, culture*. Tessellations Publishing, Phoenix, Arizona, 2012. p. 299–306.

49 Windeknecht MB. *Color-and weave II*. Self Published, 1994.

50 Windeknecht MB, Windeknecht TG. 1980. Microcomputer graphics and color and wedge effect in handweaving. In: *ACM Southeast Regional Conference Archive, Proceedings of the 18th Annual Southeast Regional Conference*. Vol. 18. University of Arizona. p. 174–179.